

Sea urchin-like microstructures pressure sensors with an ultra-broad range and high sensitivity

Xiu-man Wang¹, Lu-qi Tao², Min Yuan¹, Zeping Wang¹, Jiabing Yu¹, Dingli Xie¹, Feng Luo¹, Xianping Chen^{*1,2} & ChingPing Wong^{*3}

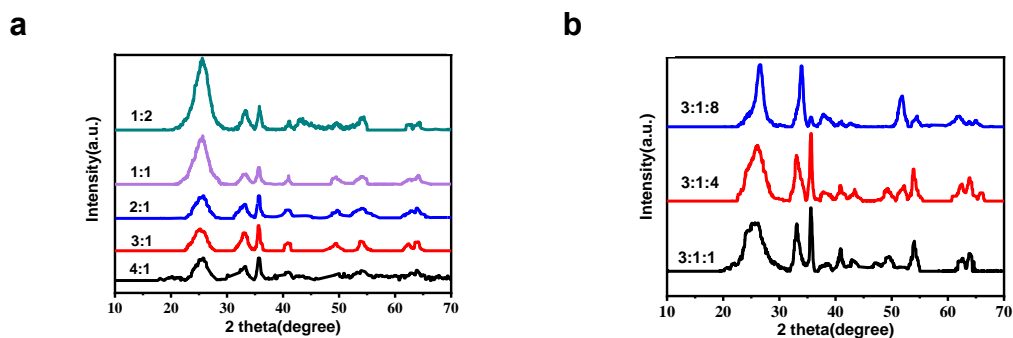
¹Key Laboratory of Optoelectronic Technology & Systems, Education Ministry of China, Chongqing University and College of Optoelectronic Engineering, Chongqing University, Chongqing 400044, China

²State Key Laboratory of Power Transmission Equipment & System Security and New Technology and School of Electrical Engineering, Chongqing University, Chongqing 400044, China.

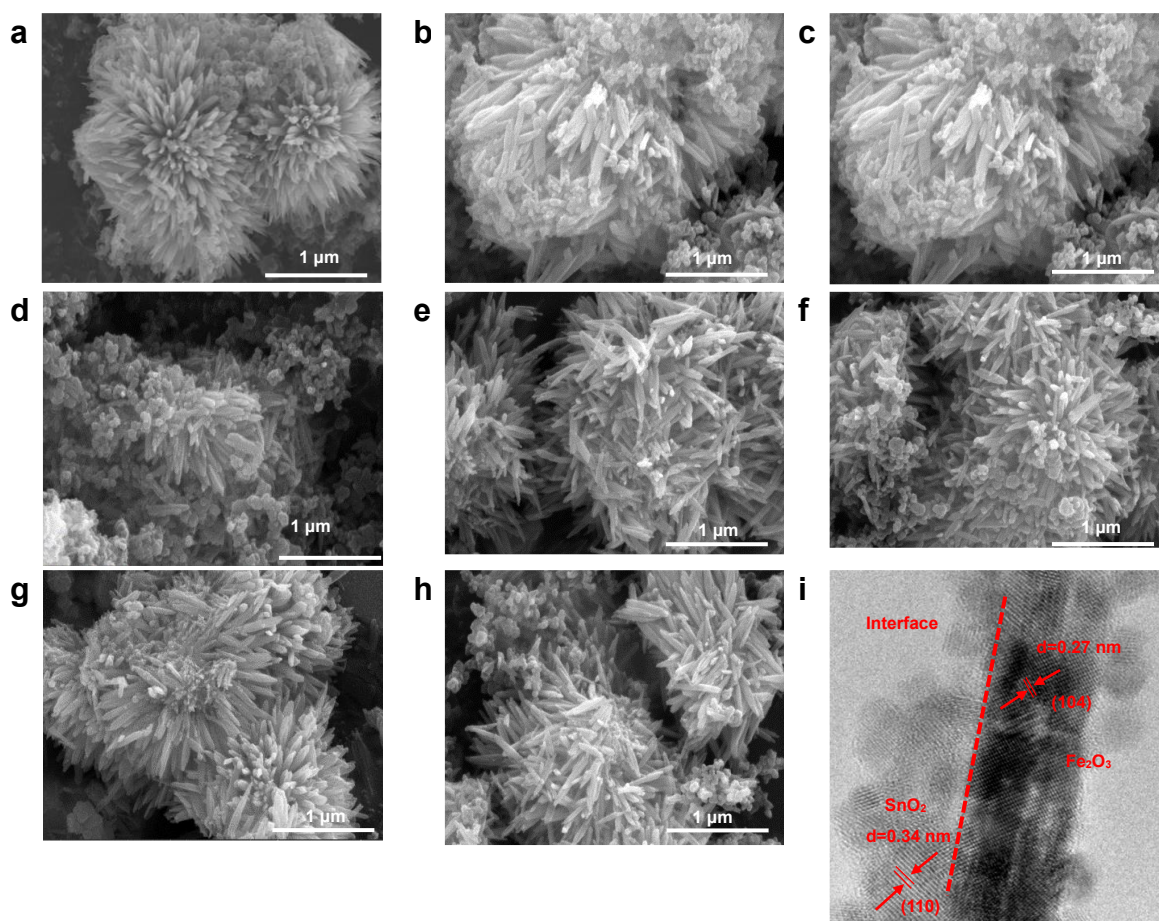
³School of Materials Science and Engineering, Georgia Institute of Technology

*Corresponding author: xianpingchen@cqu.edu.cn cp.wong@mse.gatech.edu

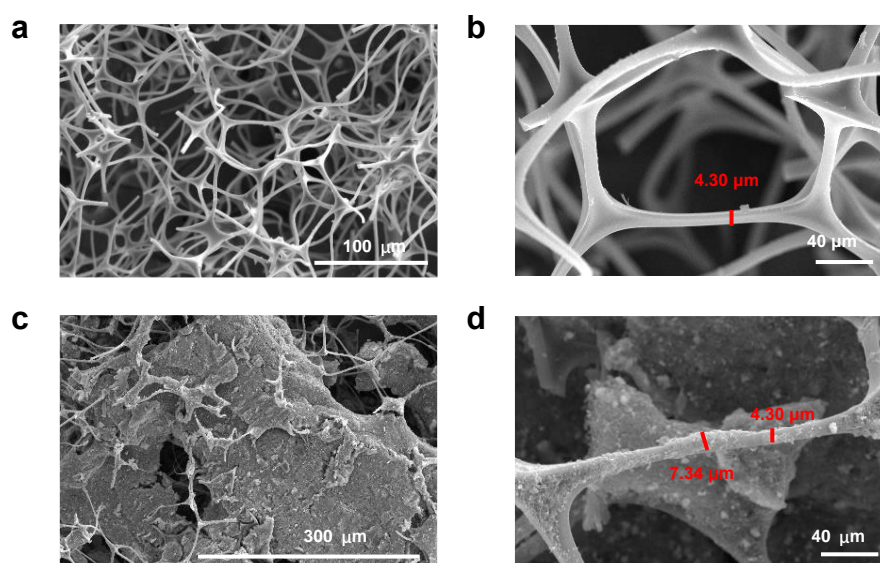
Supplementary Figures



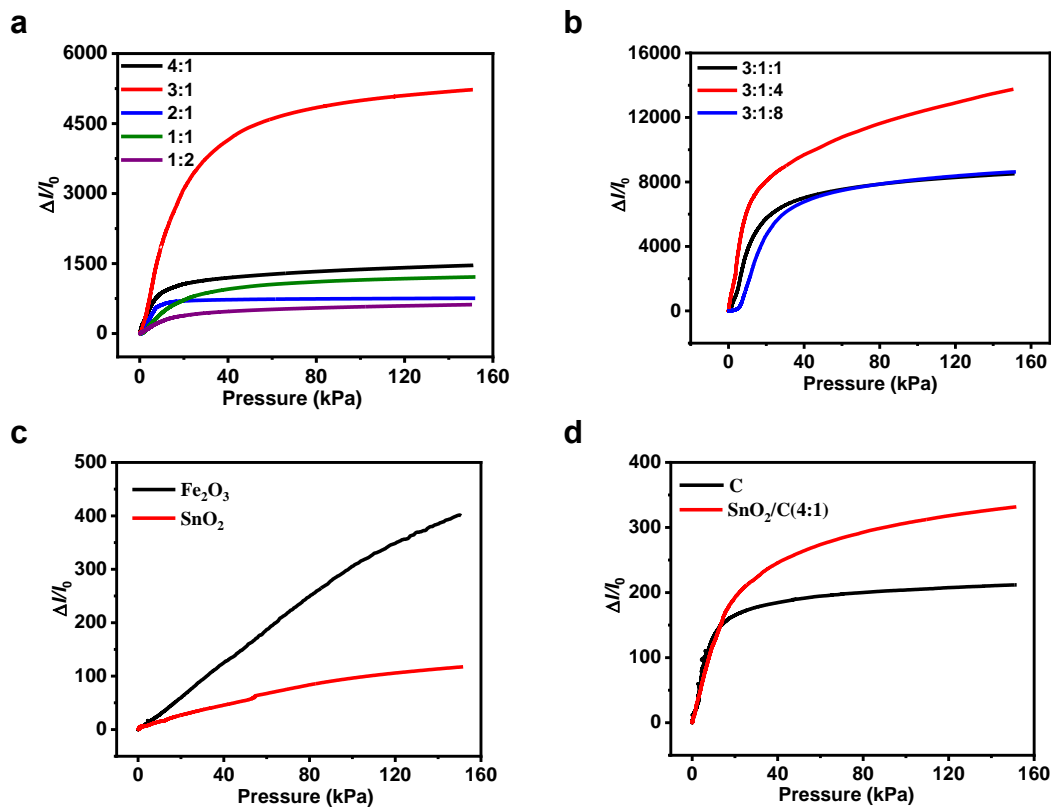
Supplementary Figures 1. XRD patterns. **a** the different mass ratios of Fe₂O₃/C (4:1,3:1,2:1,1:1,1:2), **b** the different mass ratios of Fe₂O₃/C@SnO₂(3:1:1,3:1:4,3:1:8)



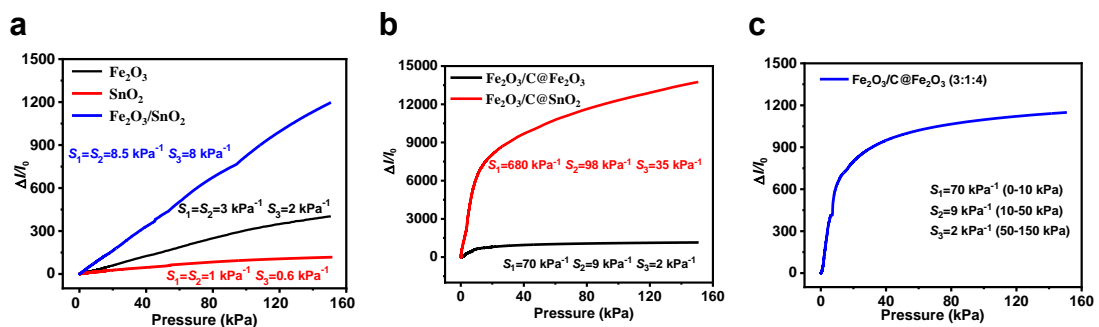
Supplementary Figure 2. $\text{Fe}_2\text{O}_3/\text{C}$ and $\text{Fe}_2\text{O}_3/\text{C}@\text{SnO}_2$ microparticle morphology. The SEM images of the different mass ratios of $\text{Fe}_2\text{O}_3/\text{C}$ (**a** 4:1, **b** 2:1, **c** 1:1, **d** 1:2), the different mass ratios of $\text{Fe}_2\text{O}_3/\text{C}@\text{SnO}_2$ (**e** 3:1:1, **f** 3:1:8, **g** 3:1:4), **g** and **h** the mass ratio of Fe_2O_3 , C, and SnO_2 3:1:4 after loading-unloading for 3500 cycles. **i**. High resolution TEM(HRTEM) images of the mass ratio of Fe_2O_3 , C and SnO_2 3:1:4.



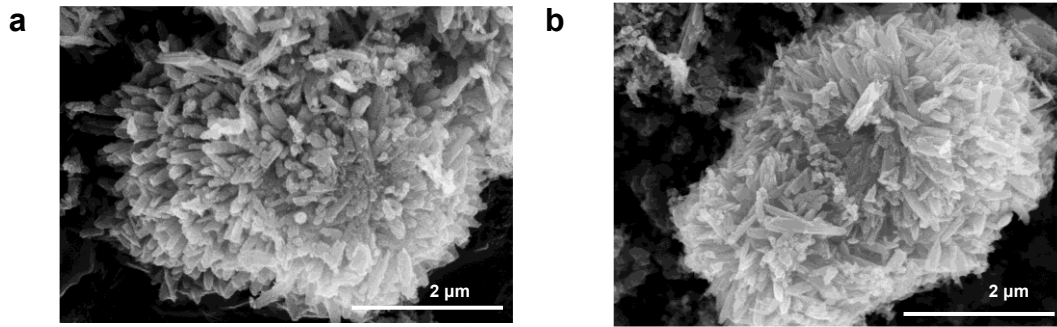
Supplementary Figure 3. SEM images. **a** and **b** SEM images of melamine sponge, **c** and **d** SEM images of $\text{Fe}_2\text{O}_3/\text{C}@\text{SnO}_2/\text{melamine}$ sponge.



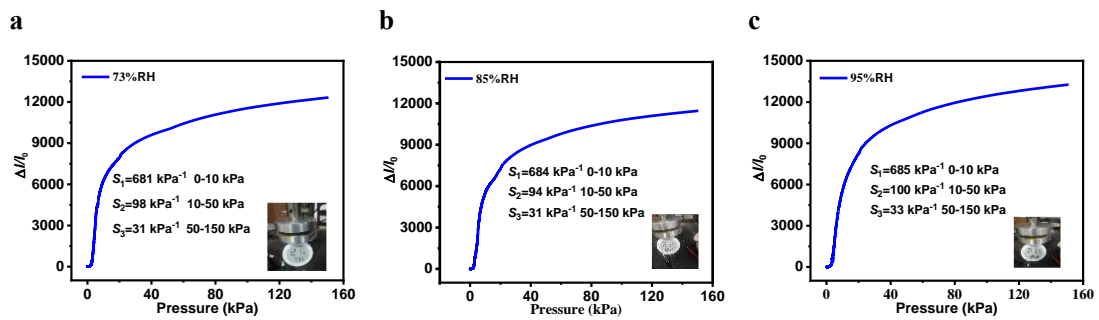
Supplementary Figure 4. Pressure-sensing characterizations. **a** Relative current change for the applied pressure, where the curves represent the different mass ratios of $\text{Fe}_2\text{O}_3/\text{C}$ (4:1, 3:1, 2:1, 1:1 and 1:2), **b** The different mass ratios of $\text{Fe}_2\text{O}_3/\text{C}@/\text{SnO}_2$ (3:1:1, 3:1:4 and 3:1:8), **c** Fe_2O_3 and SnO_2 , **d** C and the mass of SnO_2/C 4:1.



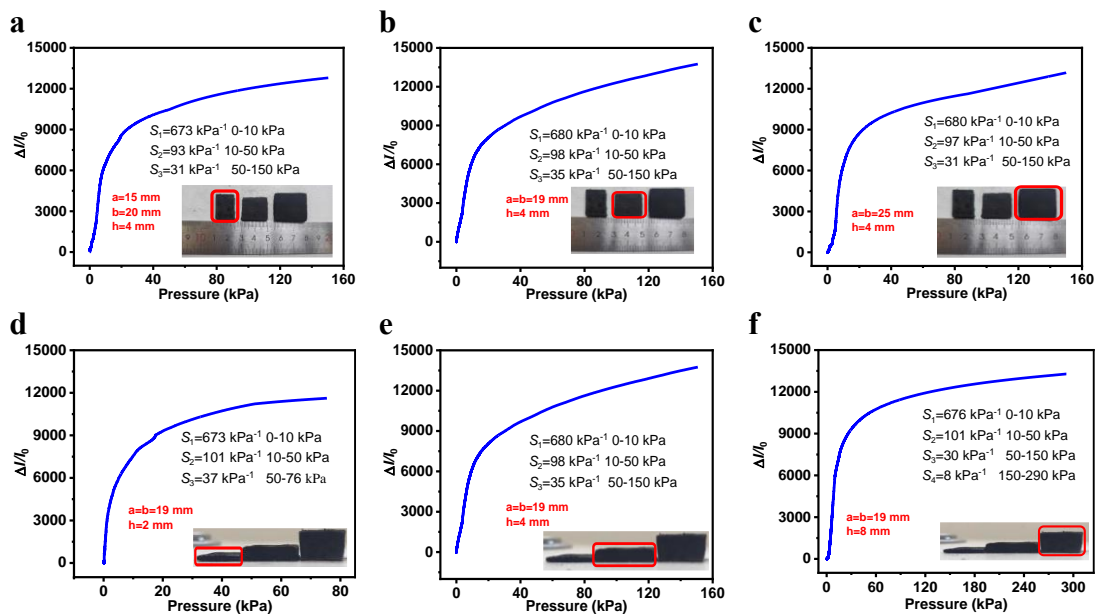
Supplementary Figure 5. Pressure-sensing characterizations. **a** The sensitivity of Fe_2O_3 , SnO_2 , and $\text{Fe}_2\text{O}_3/\text{SnO}_2$ pressure sensor. **b** The sensitivity of $\text{Fe}_2\text{O}_3/\text{C}@/\text{Fe}_2\text{O}_3$ (3:1:4) and $\text{Fe}_2\text{O}_3/\text{C}@/\text{SnO}_2$ (3:1:4) pressure sensor. **c** The sensitivity of $\text{Fe}_2\text{O}_3/\text{C}@/\text{Fe}_2\text{O}_3$ with the mass ratio of 3:1:4 based sensors.



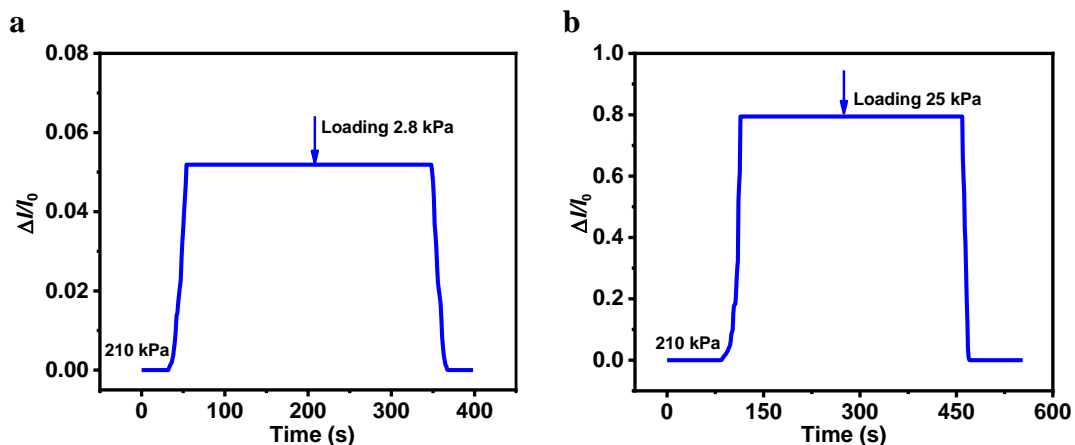
Supplementary Figure 6. SEM images of $\text{Fe}_2\text{O}_3/\text{C}@ \text{Fe}_2\text{O}_3$ (3:1:4)



Supplementary Figure 7. Sensing performance under different relative humidity. Sensitivities of $\text{Fe}_2\text{O}_3/\text{C}@ \text{SnO}_2$ (3:1:4) pressure sensor under the RH of **a** 73%, **b** 85% and **c** 95% at room temperature.



Supplementary Figure 8. Sensing performance under different areas and thickness. The current ratio variation with pressure of the $\text{Fe}_2\text{O}_3/\text{C}@ \text{SnO}_2$ (3:1:4) sponge **a-c** with a sizes of 15×20 mm, 19×19 mm and 25×25 mm, **d-f** thickness of 2 mm, 4 mm and 8 mm, respectively.



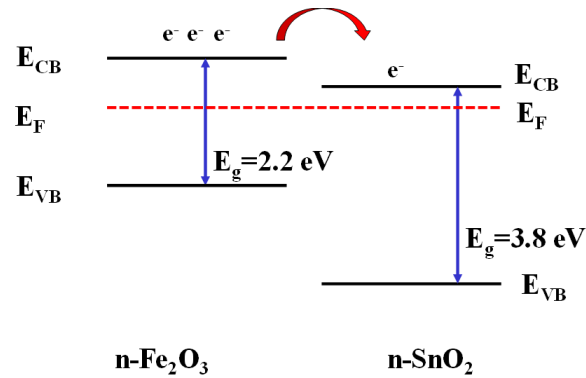
Supplementary Figure 9. Detection of micro pressure under loading pressures. **a** 2.8 kPa and **b** 50 kPa.

Supplementary Table 1 Sensitivity summary of pressure sensor in this work

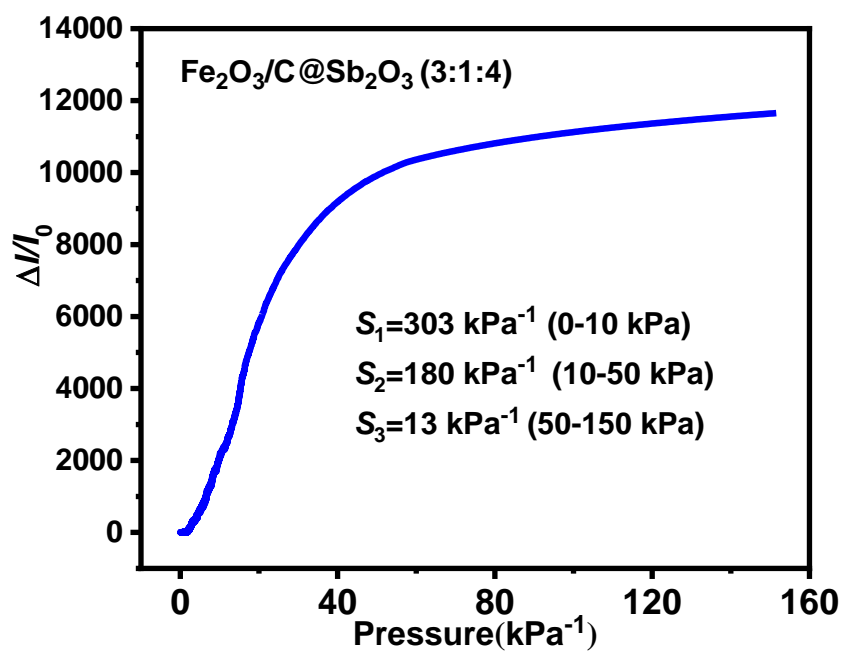
Materials	Sensitivity(kPa^{-1}) (0-10 kPa)	Sensitivity (kPa^{-1}) (10-50 kPa)	Sensitivity (kPa^{-1}) (50-150 kPa)
Fe_2O_3	3	3	2
SnO_2	1	1	0.60
C	15	0.88	0.20
$\text{Fe}_2\text{O}_3/\text{C}$ (4:1)	88	7	2.30
$\text{Fe}_2\text{O}_3/\text{C}$ (3:1)	203	44	6
$\text{Fe}_2\text{O}_3/\text{C}$ (2:1)	76	9	3.90
$\text{Fe}_2\text{O}_3/\text{C}$ (1:1)	47	8	1.27
$\text{Fe}_2\text{O}_3/\text{C}$ (1:2)	28	3	1.02
SnO_2/C (4:1)	13	2.4	0.7
$\text{Fe}_2\text{O}_3/\text{C}@/\text{SnO}_2$ (3:1:1)	420	80	12
$\text{Fe}_2\text{O}_3/\text{C}@/\text{SnO}_2$ (3:1:4)	680	98	35
$\text{Fe}_2\text{O}_3/\text{C}@/\text{SnO}_2$ (3:1:8)	314	65	11

Supplementary Table 2 Sensitivity summary of pressure sensor in reference

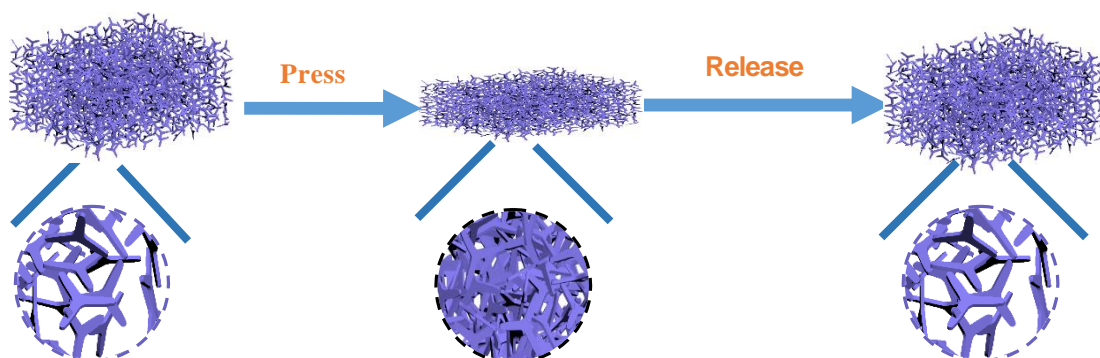
Materials	Nanostructure	Sensitivity (kPa^{-1})	Reference
ZnO/PDMS	Sea urchin-like	75 - 121 (0 - 200 Pa)	1
Au/Ag/PU	Sea urchin-like	2.46 (0 - 1 kPa) 0.52 (1 -8.2 kPa)	2
C/PDMS	Sea urchin-like	263 at 1 Pa	3
Mxene/Reduced Graphene Oxide Aerogel	Naosheets	0.55 (23 - 982 Pa) 3.81 (982Pa - 10 kPa) 2.52 (10 - 30 kPa)	4
Carbon Black@Polyurethane Sponge	Nanosheets	0.068 (0-2 kPa) 0.023 (2-10 kPa) 0.036 (10-16 kPa)	5
MXene/Sponge	Nanosheets	147 (0-5 kPa) 442 (5-20 kPa)	6
Graphene/Eco-flex	Triode-mimicking	4.68 (0-150 kPa) 11.09 (150-200 kPa)	7
CNT/cotton textile	Nanowires	14.4 (0-3.5 kPa) 7 (3.5-15 kPa)	8
MXene/tissue paper	Nanosheets	0.55 (0-3 kPa) 3.81 (3-10 kPa)	9
$\text{Fe}_2\text{O}_3/\text{C}@\text{SnO}_2/\text{Sponge}$	Sea urchin-like	680 (0-10 kPa) 98 (10-50 kPa) 35 (5-150 kPa)	In this work



Supplementary Figure 10. Schematic illustration of formed $\text{Fe}_2\text{O}_3\text{-SnO}_2$ n-n heterojunction. E_{CB} : conduction band edge energy, E_{VB} : valence band edge energy, E_{gap} : band gap energy, E_{F} : fermi energy.



Supplementary Figure 11. Change of current with pressure increases for Fe₂O₃/C@Sb₂O₃.



Supplementary Figure 12. The schematic pressure-sensing models of the sponge.

Reference

1. Yin, B., Liu, X., Gao, H., Fu, T., & Yao, J. Bioinspired and bristled microparticles for ultrasensitive pressure and strain sensors. *Nat. Commun.* **9**, 1-8 (2018).
2. Lee, D. et al. Highly sensitive, transparent, and durable pressure sensors based on sea-urchin shaped metal nanoparticles. *Adv. Mater.* **28**, 9364-9369 (2016).
3. Shi, L. et al. Quantum effect-based flexible and transparent pressure sensors with ultrahigh sensitivity and sensing density. *Nat. Commun.* **11**,1-9 (2020).
4. Ma, Y. et al. 3D synergistical MXene/reduced graphen oxide aerogel for a piezoresistive sensor. *ACS Nano*, **12**, 3209-3216 (2018).
5. Wu, X. et al. Large-Area Compliant, Low-Cost, and Versatile Pressure-Sensing Platform Based on Microcrack-Designed Carbon Black@Polyurethane Sponge for Human-Machine Interfacing. *Adv. Funct. Mater.* **26**, 6246-6256 (2016).
6. Yang, Y. et al. 3D hybrid porous Mxene-sponge network and its application in piezoresistive sensor. *Nano Energy*. **50**, 79-87 (2018).
7. Wu, Q. et al. Triode-mimicking graphene pressure sensor with positive resistance variation for physiology and motion monitoring. *ACS Nano*. **14**, 10104-10110 (2020).
8. Liu, M. et al. Large-Area All-Textile Pressure Sensors for Monitoring Human Motion and Physiological Signals. *Adv. Mater.* **29**,701-709 (2017).
9. Ying, et al. A Wearable Transient Pressure Sensor Made with MXene Nanosheets for Sensitive Broad-Range Human-Machine Interfacing. *Nano lett.* **19**, 1143-1150 (2019).